Conference Paper, Published Version

Malekpour, Ahmad; Karney, Brian; St-Aubin, Richard; Radulj, Djordje

Exploring the Underlying Physics of the Double Vortex Insert Device by CFD

IWLHS, 20-22/02/2013, Aachen - Bung & Pagliara (eds) - © 2013 Bundesanstalt für Wasserbau ISBN 978-3-939230-04-5

Exploring the Underlying Physics of the Double Vortex Insert Device by CFD

A. Malekpour & B. Karney
University of Toronto, Toronto, Canada

R. St-Aubin
IPEX Inc., Toronto, Canada

D. Radulj
HydraTek & Associates Inc., Toronto, Canada

ABSTRACT: The "double vortex" is a patented device originally invented by Dr. Eugene Natarius in order to efficiently admit and mix air into sewer systems. Examination of the general flow pattern via both a conceptual and CFD model revealed that this device does indeed possess considerable potential to admit and mix a large amount of air. This study explores and seeks to understand the flow mechanism through which air is admitted and mixed. To this end, the program Fluent is utilized to perform a three-dimensional two-phase flow analysis. Numerical experiments show that the device's elbow shape establishes a negative pressure at a high point inside the device, and that this mechanism is mainly responsible for admitting air into the system, while its double vortex rotation by enhancing water and air mixing assists in downstream air movement. The negative pressure is primarily induced by the profile that causes the hydraulic grade line to fall below the pipe's centerline. To better understand the original device, the alternative of a simple elbow with an air vent to admit flow to the top of a drop shaft is also numerically investigated. The results show that this simple assembly also admits considerable amount of air into the system through the same mechanism, although the large quantity of air intrusion constraints the flow and causes air to partly separate from the water flow.

Keywords: Double Vortex, Aeration, Sewer System, CFD

1 INTRODUCTION

In general, vertical drop shafts are commonly used as compact hydraulic structures that safely connect a higher energy flow upstream to a lower downstream energy level. These structures at least partly function as energy dissipators where an annular hydraulic jump forming at the bottom of the shaft is a key component in this mechanical energy dissipation. Moreover, in wastewater systems they also function as an aerator to increase the oxygen dissolved in the wastewater, which in turn helps to alleviate pipe corrosion and odour problems (Natarius 2000).

The most important opportunity and challenge of these structures is the formation of large air pockets in the vertical water column resulting from chaotic shaft water motion, which is then forced into the downstream conduit. Air pocket that coalesce in the downstream conduit is often problematic and may result in intermittent flow or even blowback if the buoyancy force acting on the air pocket exceeds the flow-induced drag force (Falvey 1980). Moreover high levels of flow agitation in these structures enhance the emission of hydrogen sulphide (H_2S), which could worsen odour issues locally (Churchill and Elmer 1999).

To cope with the problems associated with vertical drop shafts, an innovative device like the vortex drop structure with the Vortex Insert Assembly (VIA) was developed by Dr. Eugene Natarius (Natarius 2000). The VIA is a simple, pre-fabricated insert for existing or new drop structures. It has been shown to appreciably reduce odour and corrosion issues on all types of sewer drops.

Recently a new type of drop shaft with a Double Vortex Inlet (DVI) assembly was proposed by the same inventor to improve the performance of the VIA. This assembly works with fully pressurized flow and is believed to require a lower drop height in order to perform well and to achieve the desired results. Although this new assembly has not been field tested, the observations made on the performance of a

small-scale physical model revealed good potential for sewer aeration and that the device could be effectively employed to alleviate the odour and corrosion issues in sewer systems. Unfortunately, little is presently known about the underlying physics driving the direct air entry into the system, which in turn complicates the setup of the design criteria for real applications and sometimes leaves designers leery to try something that they do not completely understand. Thus, this study aims to shed light on the mechanism under which air could be sucked or drawn into the system. A better understanding of the underlying physics would make it easier to refine and apply design criteria for field applications.

A brief overview of the mechanism governing the traditional vortex inlet drop shaft is a good departure point toward the physical understanding of DVI drop shaft structure.

2 VORTEX INLET DROP SHAFTS

A typical schematic of a (single) vortex inlet drop structure is shown in Figure 1. The open channel flow approaching the structure contracts at the entrance by passing into the region of reduced cross-sectional area. This section is designed such that a flow control section is established at the entrance. The critical flow section hydraulically isolates the effluent system from the performance of the drop shaft structure. The flow passing through the control section switches from subcritical in the effluent conduit to supercritical in the steep-sloped vortex channel where the flow is accelerated to achieve the required vortical strength. The vortex flow causes the water to cling to the drop shaft's walls and produces a well-defined and stable air cone at the middle of the shaft. In such a design, the air column is not blocked anywhere between the upstream and downstream ends of the vertical shaft, and thus large scale air intrusion to the downstream conduit is avoided. Moreover, the vertical velocity of the water column motivates slight negative pressures that in turn induce a weak air flow below the shaft. This flow can effectively limit the development of unfavourable odours. The vortex nature of the flow also causes an inner pressure gradient to be established just below the downstream water surface, and this is directly due to the annular hydraulic jump. The inward pressure gradient causes the air bubbles to move to the center of the shaft and thus leaves the water to the air cone (Zhao et al. 2006). Another important superiority of the vortex drop shaft over plunge-flow models is the enhancement and predictability of energy dissipation in the vortex drop as the flow clings to the wall and gives rise to skin friction loss (Jain 1988). Although the energy loss is less than that produced by the annular hydraulic jump, it can still reduce the force imposed by the fluid on the bottom face of the drop shaft. In summary, vortex inlet drop structures can appreciably reduce odour and corrosion problems in sewer systems through increasing the oxygen dissolved in the sewer flow, and by reducing the turbulence-based agitation in the drop structure (Moeller and Natarius 2000).

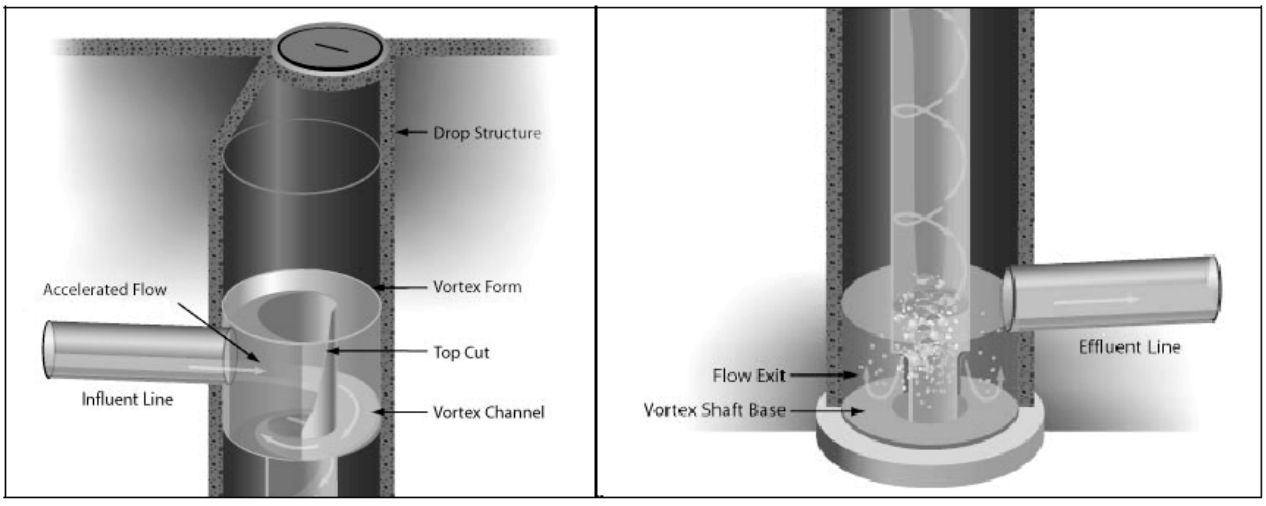

Figure 1. Typical vortex inlet drop shaft (left- inflow; right-outflow)

3 DOUBLE VORTEX INLET DROP SHAFT

The double vortex inlet drop shaft (hereafter often referred to as DVI), is naturally related to the device just described in the previous section, but it also differs from it in several key ways as well. First, the new device is designed to work under fully pressurized flow and it is believed to require a lower drop height in order to perform as designed. Unfortunately, little information is presently available regarding the performance of the DVI structure, with the exception of a video showing a small-scale model of the device. The track/path of the flow in the structure/system can be explained by considering geometrical drawings of the double vortex inlet device (Figure 2).

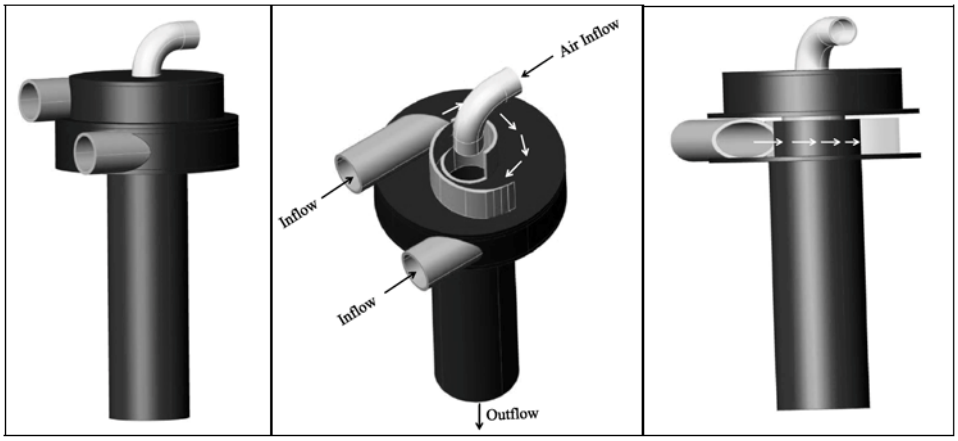

(A) (B) (C)

Figure 2. Three dimensional geometrical model of DVI: (A) general view, (B) flow path in upper chamber, and (C) flow path in lower chamber

The effluent conduit is split into two pipes at the entrance of the device and each pipe then feeds a distinct chamber in such a way that the flow in the upper chamber rotates in the opposite direction to the flow in the lower chamber. The upper chamber flow is discharged to a sinkhole at the chamber's center where the flow is delivered to a vertical pipe collecting the flow from the lower chamber. An air vent at the top of the upper chamber admits air into the system.

The experiments made on a small scale model of the DVI drop shaft show that the device does admit the desired large quantity of air into the system; however, the air intrusion mechanism has never actually been properly explained and/or documented. Figure 3 presents a few snapshot pictures from a video demonstrating the performance of the model device. The flow is completely air free when the air vent is plugged (left picture) whereas it develops a bubbly flow with its characteristic milky colour once the air vent is unplugged (right picture).

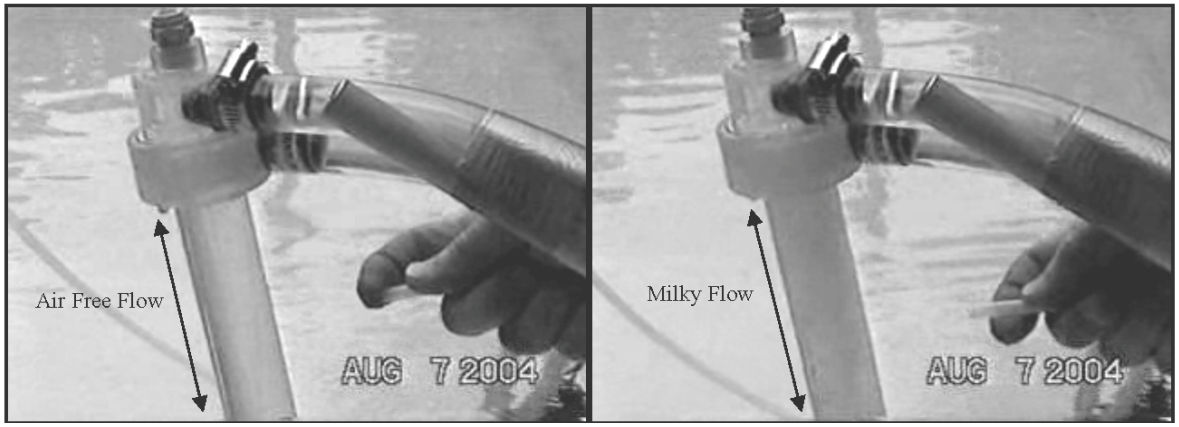

Figure 3. DVI device performance pictures

The key question that arises is whether the double vortex created in the chambers is responsible for the significant air intrusion, or whether or not other factors/mechanisms are at play. Certainly, the pressure in the upper chamber is obviously less than atmospheric since it allows air into the system. The next question is therefore whether the double vortex formation in the chamber can produce negative pressures in the upper chamber, or whether any other mechanism induces the sub-atmospheric pressure at that point.

To answer this crucial question, one should first consider the operational circumstances under which the negative pressures could be induced in such a pipe system.

4 ORIGINS OF NEGATIVE PRESSURE

Negative or sub-atmospheric pressures can be induced in closed conduit systems under two fundamentally different conditions. First, it can occur if the system velocity locally increases due to a decrease in the cross-sectional area. The velocity at which the negative pressure is created depends on the system pressure and flow conditions; the higher the original pressure, the higher the required velocity. An example of this phenomenon is the pressure drop at the throat of a venturi tube in which the velocity increase gives rise to a pressure reduction.

The negative pressure at the throat section can more easily be achieved when the upstream pressure decreases due to a velocity increase in the throat section. The simple mechanism of a venturi has made it an ideal device for the injection of Chlorine or other gases into closed conduit pipe systems. This mechanism is also useful for water pipe system aeration. Baylar et al. (2009) experimentally measured the amount of air that intrudes into a venturi tube through the orifices installed at the throat. These authors found that the device can perfectly admit air to the system provided that a negative pressure is established in the throat section. However, this device can really only be implemented low pressure pipe systems because in the case of high pressure systems, the velocity required to bring the hydraulic grade line (HGL) below the throat's elevation is typically impractically high.

The second condition that could potentially induce a negative pressure in a pipe system occurs when the HGL falls below the pipeline elevation profile. As an example, in a sufficiently long gravity system where the pressure at the outlet section is equal to the atmospheric pressure, the HGL in the pipe system can be obtained with fairly good accuracy by connecting the end of the pipe to the water surface of an upstream reservoir. The HGL in such a typical pipe system that discharges water to the atmosphere through a short-vertical elbow is shown in Figure 4. As shown, the negative pressure can be expected across a wide range of the system, with the maximum negative pressure value occurring at the end of the pipe and this value is essentially equal to the height of the elbow, denoted by "h".

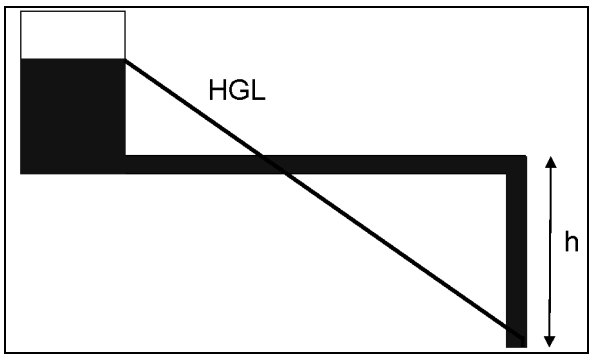

Figure 4. Negative pressure establishments in a typical pipe system

An easy way to investigate whether a high velocity is the source of the negative pressure in the double vortex device is to inspect the flow path cross-sectional area through a three-dimensional geometrical model. Figure 2 presents a geometrical model of the DVI device, as developed based on the available device prototype drawings. Flow paths are shown by arrows in the upper and lower chambers, and it is relatively clear that the potential flow cross-sectional area in the chambers is not reduced when compared to the pipes feeding the chambers. Although non-uniform flow distribution caused by the vortex action in chambers may still increase the velocity beyond that of the entrance pipes, the vortex flow is not strong enough to give rise to a considerable velocity increase. This can be easily shown by applying the free vortex concept on the simplified flow pattern inside the chambers, as shown in Figure 5.

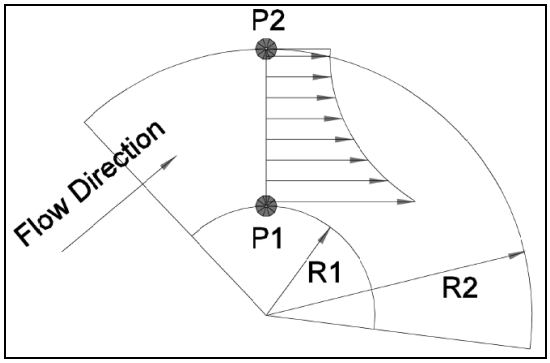

Figure 5. Schematic velocity distributions inside the double vortex chambers

The free vortex flow assumption insists that the production of tangential velocity and curvature radius of flow is constant, such that:

$$VR = C \tag{1}$$

In the current case, the constant on the right hand side of the above equation can be easily calculated by applying the mass conservation law. The flow through the section P1-P2 can be calculated by the following equation:

$$Q_{P1-P2} = \int_{R1}^{R2} VHdr = \int_{R1}^{R2} \frac{HCdr}{r} = HC \ln\left(\frac{R_2}{R_1}\right) \tag{2}$$

where H = the height of chamber, $R1$, $R2$ = the radius of inner and outer chamber walls, C = vortex constant value, V = tangential velocity, R = streamline curvature radius.

Mass conservation requires that the flow passing through section P1-P2 is exactly equal to flow entering the system via the inlet pipe. Therefore, the constant coefficient, C, can be calculated as follows:

$$C = \frac{Q_I}{H \ln\left(\frac{R_2}{R_1}\right)} = \frac{\pi D^2 V_I}{4H \ln\left(\frac{R_2}{R_1}\right)} \tag{3}$$

where Q_I = inlet pipe discharge, V_I = inlet pipe velocity, and D = inlet pipe diameter.

The above equation can be applied on the given example in order to investigate how the velocities change inside the chambers. To this end, a DVI is considered with: D = 7.5 cm, upper chamber R1 and R2 = 5, and 15 cm respectively, lower chamber R1 and R2 = 7.5, and 17.5 cm respectively, upper and lower chamber H = 7.5 cm. With this information the maximum velocities inside the upper and lower chambers for different inlet velocity are calculated by using Equations 1 to 3, and the results are summarized in Table 1.

As shown, the velocities in the upper chamber are just slightly greater than the inlet velocity, whereas the velocities in the lower chamber are lower than the inlet velocity. It is evident that such velocity changes cannot be responsible for the negative pressure and air intrusion to the system, particularly when the extra turbulence induced by the interaction of the opposite rotating flow in the chambers that is not considered in this simplified approach, acts to make the velocity field more uniform. While this is partially evident in the simple model, a more precise determination of the cross-sectional flow area is more readily obtained through the use of a three-dimensional numerical analysis via computational fluid dynamics (CFD).

Table 1. Maximum velocity in upper and lower chambers

Inlet velocity (m/s)	Maximum velocity in upper chamber (m/s)	Maximum velocity in lower chamber (m/s)
2	2.14	1.85
3	3.22	2.78
4	4.30	3.70
5	5.36	4.63
6	6.44	5.56

Based on hydraulic laws, the provisional conclusion at this point is that the significant air intrusion into the DVI is likely primarily due to the device's elbow shape profile rather than the direct action of the swirling flow formed in the chambers. A CFD analysis is an excellent tool for confirming this concept because it can act to provide a precise velocity field within the DVI; information from which it is subsequently possible to justify the conclusions obtained from the simplified analysis. Furthermore, if the elbow shape of the DVI is the dominant cause of air intrusion, a CFD analysis of both a DVI and a simple elbow with an air vent at the top, should ultimately yield similar results.

5 CFD ANALYSIS

5.1 *Governing physics and employed model*

The device's geometry ensures that the true flow pattern in the system has strong three-dimensional characteristics and thus that pattern could be determined by a three dimensional hydraulic analysis, in which all flow channels formed by internal and external walls of the device must be considered. Moreover, in order to consider the air flow in the system, a two phase flow model is also critical.

Generally speaking, several different types of two phase flow regimes can potentially occur in systems, including bubbly flow, droplet flow, slug flow, and stratified flow (Falvey 1980). Visual observations of the double vortex device (see Figure 3) reveal that air does indeed move within the system and this is most evident through the presence of the large number of small and diffused bubbles. Several different types of two phase flow models exist, including: the volume of fluid (VOF), Eulerian, and mixed flow models. The mixed flow model is the most compatible model that can be used to resolve bubbly flow motion and therefore is the preferred and employed model for this study. This numerical approach can model the water and air phases by solving momentum and continuity equations for mixture, the volume fraction equation for the air phase, and the algebraic expressions for the relative velocity.

In this research the proven CFD software, Fluent V6.3 (Fluent Inc. 2006), is employed as the numerical tool of choice. A three dimensional algebraic model with slip velocity and with the standard k-ε turbulence model is selected as the computational model within Fluent.

5.2 *Numerical results*

A DVI device with the same properties discussed in the simplified hydraulic analysis is directly considered within the CFD analysis. A vertical pipe with an internal diameter of 15 cm and a height of 1.5 m is assumed to collect water at the bottom of the lower chamber. The air vent size is 5 cm and the operating flow rate is assumed as 17.7 L/s, such that the velocity in each inlet pipe is 2 m/s. For the sake of comparison, the internal diameter, vertical height, air vent diameter, and flow rate for the simple elbow model are considered to be similar to those assumed for the DVI device. With this assumption, the entrance velocity to the elbow is 1 m/s.

In order to observe the hydraulic performance of the two different devices, a hydraulic model without ventilation is first considered. In order to achieve this effect the air vent surface is blocked in both cases, and a three dimensional hydraulic analysis is carried out for each case. Subsequently and in order to examine the potential for air intrusion and mixing, the air vent surfaces are unblocked and a two phase flow model simulation is carried out for each case. The following sections discuss these two sets of numerical results.

5.2.1 *Without ventilation*

To examine the hydraulic performance of the system in the absence of air intrusion, both the DVI device and the simple elbow device were simulated in the single phase mode by considering the ventilation surfaces as isolated walls. In order to verify that a velocity increase in the upper and lower chambers of the DVI is not the main cause of the induced negative pressure and subsequent air intrusion, the velocity fields in the upper and lower chambers were inspected and are shown in Figure 6. It can be seen that in general velocities in the upper chamber are higher than those in the lower chamber, and this is also predicted by the analytical model (see Table 1). Furthermore, it is evident that the velocities in both chambers do not significantly exceed the entrance velocity of 2 m/s; a result which is again in line with the analytical results. Figure 6 shows that the velocities in both chambers increase with the distance away from the outer wall and closer to the inner walls. This confirms our earlier assumption that the free vortex

motion is dominant within the chambers. Overall, the numerical results confirm that the velocity change is in itself not high enough to induce negative pressure and the air intrusion into the DVI device.

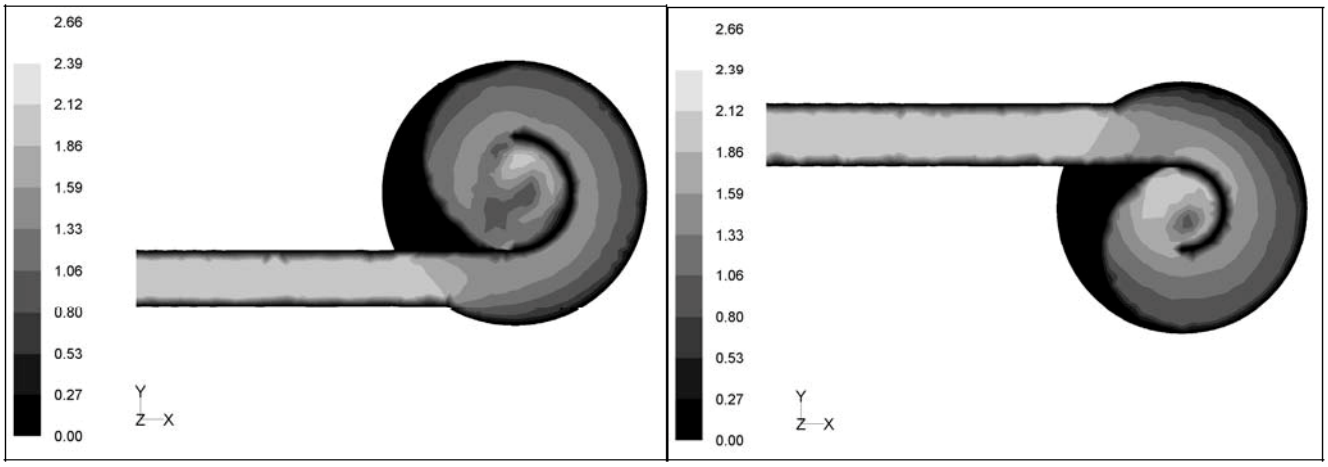

Figure 6. Velocity fields (in m/s) in the lower chamber (left) and upper chamber (right) of the DVI device

An inspection of the pressure distribution along both the DVI and the simple elbow devices reveals that the shape of the profile is likely the key cause of the negative pressures. Figure 7 depicts the predicted pressure distribution along the simple elbow and DVI devices. As shown, negative pressures having the same distribution are evident in both devices. As expected, the negative pressures increase as one moves vertically upwards towards the crown of each device. Since the velocities and the resulting head losses are low in both cases, the negative pressure heads at each point are almost equal to the elevation of the point relative to the elevation of the outlet section, or in other words to the height of the vertical section.

5.2.2 *With ventilation*

A two phase flow model simulation was performed for both the simple elbow and the DVI device in order to investigate the potential for air intrusion and mixing. The numerical results show that in both cases a significant amount of air is entrained into the system via the air vents. The total air flow rates that intrude into the DVI and simple elbow devices are predicted as 35.2 and 52.8 L/s respectively, and these are therefore almost 2 and 3 times higher than the system flow rate, respectively. These air flow rates produce high velocities of 18 and 27 m/s within the vent pipes of the DVI and simple elbow devices, respectively. Thus, not surprisingly, a small vent pipe could be used to create a flow restriction that could limit the air flow into the DVI. In general and somewhat less expected, the predicted air flow in the simple elbow is much higher than that in the DVI device. This result can be explained by considering the pressure distribution that is established within the devices, and these are shown in Figure 8.

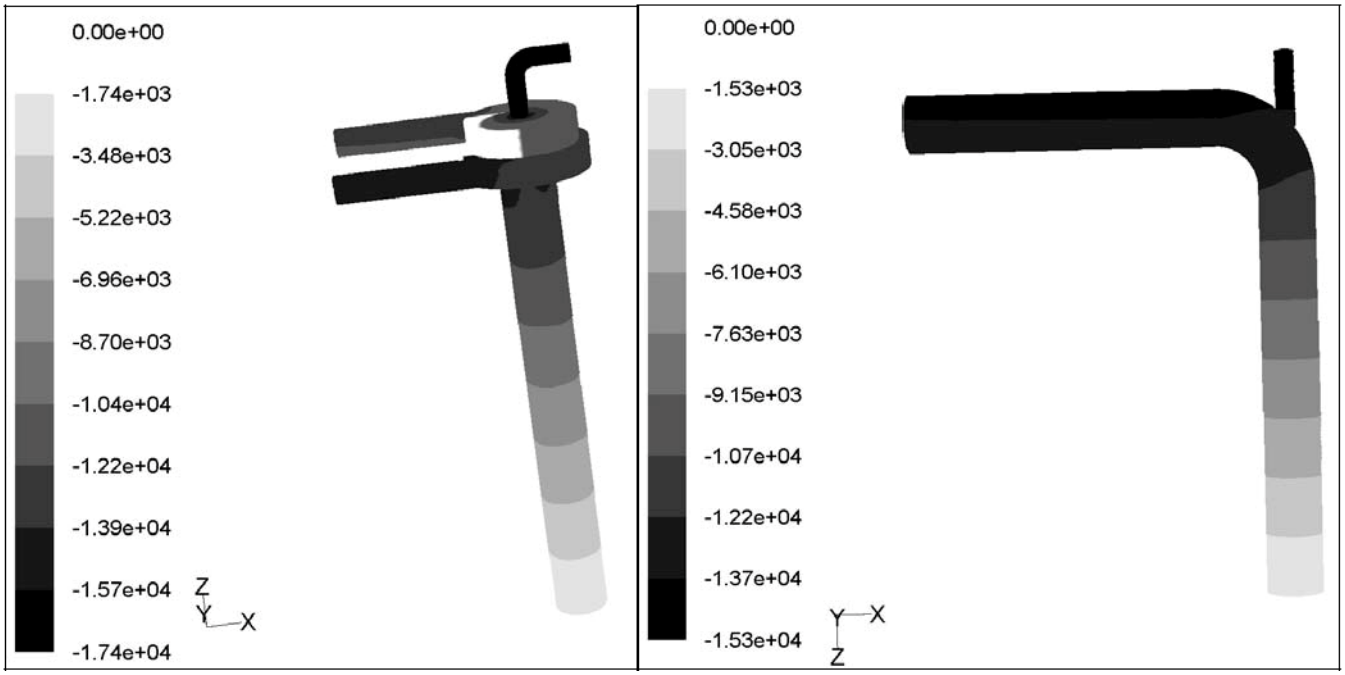

Figure 7. Pressure (in Pascals) distribution along the DVI devices, and simple elbow without aeration

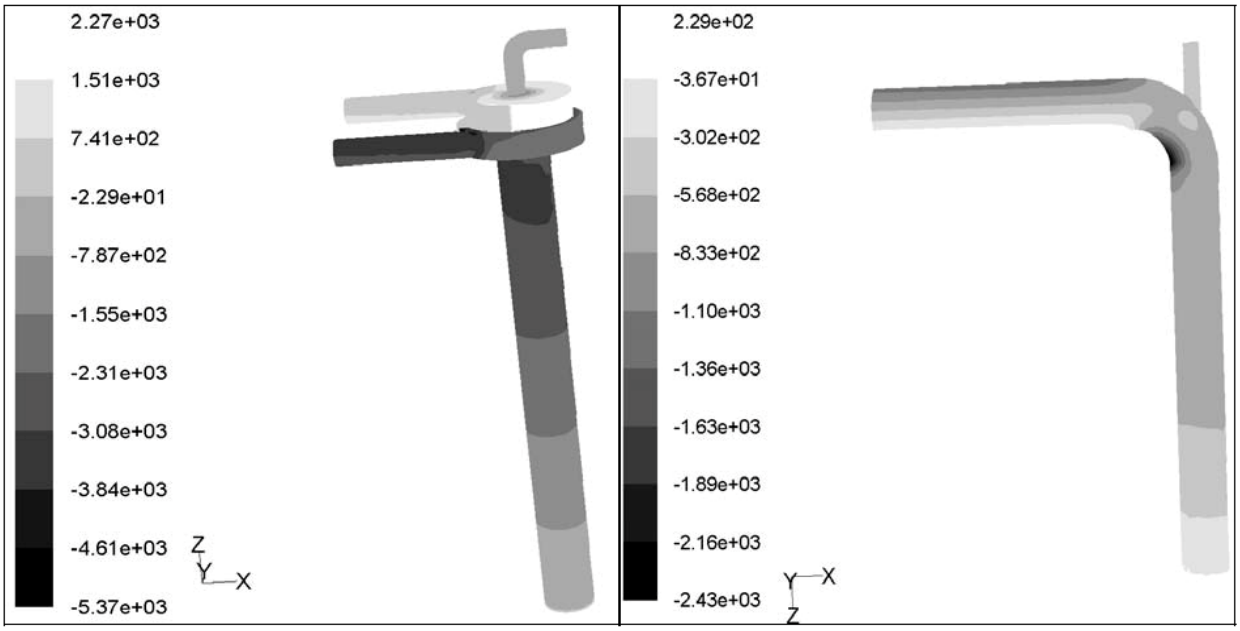

Figure 8. Pressure distributions in the DVI and simple elbow devices with aeration

As shown, the top and bottom faces of the lower chamber of the DVI experience different pressures in the range of 1510 to 714 Pa in the top face, and 741 to -22.9 Pa in the bottom face. The difference is primarily due to the head loss that occurs when the flow in the upper chamber and lower chamber are united. It is also evident that the backup pressure required to push the flow through the sink hole affects the pressure at the air vent surface. The results show that the average pressure at the air vent surface of the DVI device is -212 Pa (-0.022 m), whereas it is approximately -492 Pa (-0.05 m) at the air vent surface of the simple elbow. This small pressure difference has a significant impact on the air flow, and thus makes the simple elbow device more capable of inducing a larger air flow rate. This result is physically quite meaningful since a small vacuum pressure can yield large air flow in the air vents.

Further consideration of the pressure fields in the two devices shows that in both cases the air intrusion acts to maintain most of the pressures at almost atmospheric, although residual negative pressures still exist in both cases and are slightly greater in the DVI device because of the higher air flow in the simple elbow.

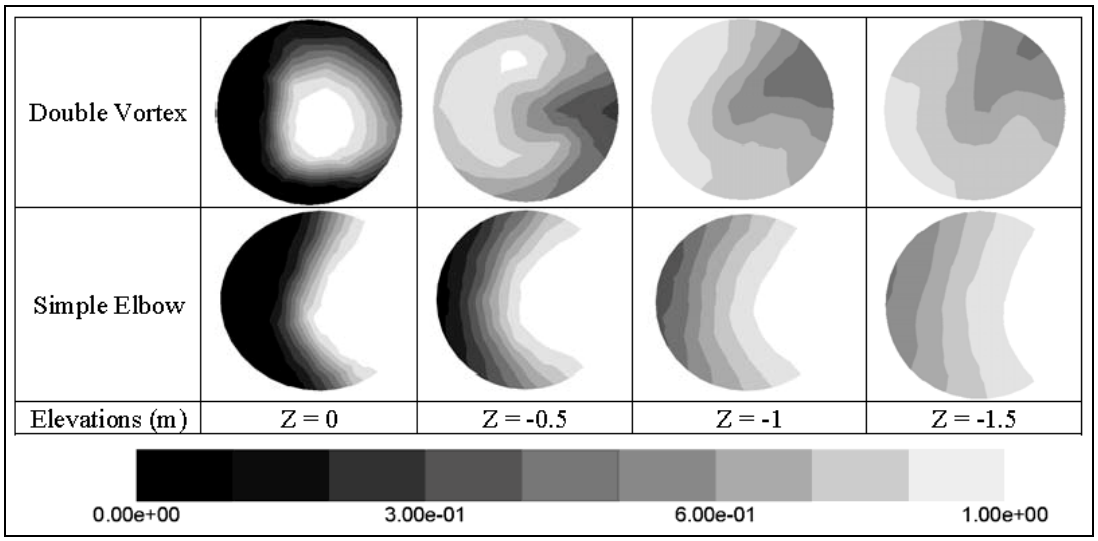

Figure 9. Air void fraction in the different cross sections of the vertical pipes of the DVI and simple elbow devices

In order to investigate the air mixing capability of the two devices, the distribution of the air void fraction across the vertical pipes was reviewed. Figure 9 compares the air void fraction across different cross sections of the vertical pipe of both devices. As can be seen at the top of the vertical pipes, the mixing is generally poor and in both cases water and air are moving in distinct layers. Air in the DVI pipe tends to flow in the middle and is also slightly deflected to the outer wall of the vertical pipe due to the action of the swirling flow. In the simple elbow case, the air flows in a distinct layer near the outer wall. Improved mixing is observed in both devices as the flow descends the vertical pipe, although in the simple elbow a

distinct air flow layer tends to moves in the outer wall of the pipe. It is also worth noting that in the DVI, the highest air void fraction zone in the cross section rotates counter-clockwise as the flow descends the vertical pipe. This is due to the swirl flow that originates at the chambers and that subsequently propagates into the vertical pipe. Furthermore, in the cross sections where the flow leaves the device (i.e., Z = -1.5 m), the air void fraction varies between 1 and 0.5 in both devices. However, in the simple elbow case, a good portion of the pure (i.e., non-mixed) air leaves the system in a single distinct layer.

Overall, the mixing appears to be better in the DVI device than in the simple elbow. Nonetheless, this fact still cannot prove the superiority of the DVI over the simple elbow, because first the amount of air flow in the simple elbow is much greater than that in the DVI and this can potentially compensate for the difference in the air form that leaves the device. Second, in both cases the air flow that enters the devices (i.e., up to 2-3 times the total system flow) significantly exceeds the amount by which air can be dissolved into water (i.e., 3-4% of the total system flow). Lastly, the overall simplicity may recommend the simple device like an elbow in some applications.

6 SUMMARY AND CONCLUSION

The performance of the double vortex insert (DVI) device is analytically and numerically explored. Using the basic hydraulic principles, it is analytically shown that the device's ability to entrain a large amount of air is due to the elbow like profile of the device, and not due to the action of swirling (vortex) flow in the chambers, as originally assumed. A 3-D CFD analysis further confirms this result. The analysis also confirms that the vortices in the upper and lower chambers are not in themselves strong enough to increase the velocities in the chambers to a level that would yield negative pressures and lead to air intrusion. Furthermore, the results confirm that the elbow shape of the device is the key component in the establishment of workable negative pressures.

In order to evaluate the air intrusion and mixing capabilities of the device, and in order to make sure that the elbow profile shape of the device is the main cause of the air intrusion, a three dimensional two phase flow analysis is performed for both the DVI device and a simple elbow with an air vent having similar geometrical and hydraulic parameters. The analysis results clearly show that both devices allow a large amount of air to intrude into the system, thereby reconfirming the crucial role of elbow shape to the DVI air intrusion behaviour. Furthermore, the results also surprisingly demonstrate that the potential air flow in the simple elbow is significant. This can be explained by considering the resulting backup pressure in the upper chamber that is established in order to compensate for the head loss that occurs when the upper chamber flow is united with the lower chamber flow within the sink hole. This backup pressure partially increases the pressure at the air vent surface which in turn causes the reduction in the air flow.

Inspection of the air void fraction in the vertical pipes of both the DVI and the simple elbow device shows that the DVI produces better mixing than the simple elbow. This is because the swirling flow that propagates from the lower chamber to the vertical pipe and more efficiently mixes the air and water, while a significant portion of air flow in the simple elbow tends to flow and leave the vertical pipe in a distinct layer and without interacting with water.

ACKNOWLEDGEMENT

The funding for this research is provided by IPEX Inc. and is gratefully acknowledged.

NOTATIONS

Q	discharge
V	velocity
R_1	the radius of the inner wall of the double vortex's chambers
R_2	the radius of the outer wall of the double vortex's chambers
H	the height of the double vortex's chambers
C	free vortex constant

REFERENCES

Baylar, A., Aydin, M. C., Unsal, M., and Ozkan, F. (2009). Numerical Modeling of Venturi Flows for Determining Air Injection Rates Using Fluent v. 6.2., Mathematical and Computational Applications, 14(2), 97-108.

Churchill, P., and Elmer, D. (1999). Hydrogen Sulfide Odor Control in Waste Water Collection Systems. NEWEA Journal, 33(1).

Falvey, H. T. (1980). Air-Water Flow in Hydraulic Structures. USBR, Denver, Colorado.

FLUENT Inc. (2006). Fluent 6.3 User Guide. FLUENT Inc.

Jain, S. C. (1988). Air Transport in Vortex-Flow Drop-Shafts. Journal of Hydraulic Engineering, 114(12), 1485–1497.

Moeller, W. P., and Natarius, E. M. (2000). The Vortex Drop Structure Inspection for Odor and Corrosion Control. WEFTEC.

Natarius, E. M. (2002). Vortex Insert Assembly Controls Odors and Corrosion in Sewer Drops, WEF Odors and Toxic Air Emissions Conference.

Zhao, C., Zho, D. Z., Sun, S., and Liu, Z. (2006). Experimental Study of Flow in a Vortex Drop Shaft. Journal of Hydraulic Engineering, 132(1), 61-68.